ANALYSIS OF ACOUSTIC SOFTENING, HEAT AND MATERIAL FLOW IN ULTRASONIC VIBRATION ENHANCED FRICTION STIR WELDING

C. S. WU*, L. SHI* and J. CHEN*

** Institute of Materials Joining, Shandong University, 250061 Jinan, Shandong, P.R. China*

DOI 10.3217/978-3-85125-615-4-29

ABSTRACT

To improve the welding efficiency and lower the welding loads in friction stir welding (FSW), a process variant of conventional FSW, i.e., the ultrasonic vibration enhanced friction stir welding (UVeFSW), is developed. The experimentations show that UVeFSW not only increases the welding speed and decrease the weld load, but also improve the microstructure and mechanical properties of the joints. To understand the underlying physics in UVeFSW, a mathematical model is developed to analyze the interaction of the ultrasonic vibration with the plastically deformed material around the tool as well as the heat transfer and material flow phenomena in UVeFSW. It is found that the ultrasonic vibration enhances the material flow and the strain rate in the shear layer, but does not cause evident temperature increment. The assistant softening in the material around the tool is caused by the exerted ultrasonic vibration, i.e., acoustic softening. The numerical analysis results lay solid foundation to explain the process effectiveness and the UVeFSW process optimization.

Keywords: Ultrasonic vibration, friction stir welding, modelling, heat transfer, material flow

INTRODUCTION

Friction stir welding process has been successful used for joining hard-to-weld aluminium alloys and for joining plates with different thickness or different materials [1]. As a solid state welding process, much less heat input is required for FSW, which leads to this process to be energy efficient, environment friendly, and versatile [2]. During FSW process, a non-consumable rotating tool with a specially designed pin and shoulder is inserted into the abutting edges of the workpieces to be joined and advancing along the abutting edges. Heat generated due to both friction and plastic deformation softened the material near the tool, thereafter, the softened material in front of the tool is transported to the trailing edge to form a joint behind the tool [3]. To generate enough heat energy to soften the material for the process, large rotational torque and plunge force are needed, so the welding equipment is large in volume, and complex clamping equipment is necessary [4]. These phenomena

are particularly severe for welding of steel and titanium alloys [5]. In addition, the high stress subjected by the tool pin causes rapid tool wear and premature tool failure which resulting in poor weld quality and high production cost [4,5]. Moreover, the high rotational torque and transverse force during FSW also limit the welding speed to a relatively low value [4].To solve these problems, some assistant heat sources (induction heat, resistance heat, laser, plasma arc, etc.) have been used to preheat the workpiece near the tool [6-8]. However, the multiple thermal cycles would cause the increasing of the volume of heat-affected zone and make the precipitated phase of the aluminium alloys tend to grow in the weld nugget zone [9,10].

The application of ultrasonic energy to the plastic deformation of metal has been widely investigated [11-13]. It has been shown that superimposing ultrasonic vibration in metal forming can reduce the yield stress and flow stress, increase the processing speed and improve the product quality [11-13]. Ultrasonic energy is an assistant heat source of low power consumption and high efficiency which can reduce the deformation resistance of material [11]. Park has employed ultrasonic vibration to the FSW tool and found that by adding ultrasonic vibrations to FSW tool results in a better weld quality, less welding force needed and increasing of the tool life [10]. Amini et al. revealed that ultrasonic vibration can reduce downward force and welding force in FSW [14]. Ma et al. performed the studies on ultrasonic assisted FSW and found that superimposing ultrasonic vibration can improve the properties of the weld joint, refine the grain and reduce the residual stress in the weld [15]. Rostamiyan et al. studied ultrasonically assisted friction stir spot welding of AA6061, and found that superimposing ultrasonic vibration in friction stir spot welding can improve lap shear force and hardness [16]. Ahmadnia et al. conducted the ultrasonic-assisted friction stir welding of AA6061 joints to analyze the effects of process parameters on the mechanical and tribological properties of joints [17]. Wu's research group have developed the ultrasonic vibration enhanced FSW (UVeFSW) system which transmits ultrasonic vibration energy directly into the workpiece near the FSW tool [9,18]. Experimental results shown that this novel UVeFSW can enhance the plastic material flow, improve the weld quality, increase the welding speed and reduce the welding loads [9,18]. In all, by adding ultrasonic vibration energy to FSW can efficiently reduce the welding loads and the residual stress, improve the weld quality and enhance the plastic fluidity of the material near the tool. However, superimposing ultrasonic vibration energy in FSW increases the complexity of the process. In order to optimize the UVeFSW and make full use of the ultrasonic vibration energy in FSW, a fundamental knowledge of the effects of superimposing ultrasonic vibration energy in FSW on thermal process and plastic material flow should be required. A rigorous numerical model coupled with experimental validation is suitable for revealing the underlying physical mechanism of UVeFSW process.

In the past decades, numerous numerical models have been reported to simulate the material flow and heat transfer in conventional FSW [19-21], but few of them are related to ultrasonic assisted FSW process. Park has simulated the ultrasonic assisted FSW by impose sinusoidal horizontal ultrasonic vibration on the tip of the FSW tool and found that the downward force decreased with increasing the amplitude of ultrasonic vibration [10]. Lai et al. established a ultrasonic assisted FSW model by considering the longitudinal ultrasonic vibration of the FSW tool as an additive inertial force and found the ultrasonic vibration can provide additional heat energy to keep sufficient welding temperature at relatively higher welding speed [22]. However, these ultrasonic assisted FSW models have

not considered the acoustic softening effect, i.e., ultrasonic energy can reduce the deformation resistance of material [23-25]. Recently, Shi et al. [26-27] developed an integrated model, which take into consideration of the ultrasonic softening and preheating effect, to analyze the effects of superimposing ultrasonic vibration on FSW process.

In order to optimize the process and the relevant microstructure and mechanical properties of the joints, a fundamental knowledge of acoustic softening, heat and mass transfer during UVeFSW process should be required. In this paper, the integrated 3D numerical model is used for quantitatively analysing the acoustic softening, heat transfer and material flow in UVeFSW process. The variation of temperature fields, material flow velocity, strain rate and viscosity under the effect of ultrasonic vibration are quantitatively analyzed to get deep insight into the underling mechanism of UVeFSW process.

EXPERIMENTAL DETAILS

Fig. 1 shows the experimental system for the self-developed ultrasonic vibration enhanced FSW (UVeFSW). The UVeFSW system can be divided into two main parts: a conventional FSW machine (FSW-3LM-003) and a self-designed device of ultrasonic vibration system. The ultrasonic vibration energy is directly transmitted into the workpiece by the sonotrode as shown in Fig. 1. Thus, the coupling of the ultrasonic energy with the friction and stirring action can produces an enhanced plastic material flow near the tool [9,18]. In this study, the ultrasonic system operates at a frequency (f) of 20 kHz and the amplitude (λ) of 40 μm during the UVeFSW process. The maximum power of the ultrasonic system is 1200 W, while the efficient power during the process is about 300 W. The distance between the center of sonotrode and the FSW too1 axis is 20 mm. The inclinations angle (φ, as shown in Fig. 2) of sonotrode with respect to the horizontal axis is 40°. The clamping force of the sonotrode is 300 N during the process.

Fig. 1 The ultrasonic vibration enhanced friction stir welding (UVeFSW) system.

Table 1 Composition of workpiece material (AA2024-T3 Al alloy) (wt, pct)

Cu	Mg	Fe	Ni	Mn	Si	Ti	Zn	Al
4.58	1.59	0.25	<0.10	0.63	0.15	<0.10	0.20	Balance

Aluminum alloy AA2024-T3 plates (300 mm in length, 80 mm in width and 6 mm in thickness) were welded in a square butt joint configuration. Table 1 lists the compositions of the workpiece materials. The shoulder diameter is 15.0 mm. The diameters of the pin at the root and tip are 5.6 mm and 3.2 mm, respectively, and its length is 5.7 mm.

MATHEMATICAL MODEL

GOVERNING EQUATIONS

UVeFSW is a complex physical process which is consisted of fully-coupled heat generation, heat transfer, material flow and ultrasonic vibration energy transmission. Only the quasi-steady state (the welding period) is dealt with in this study. The plastic material during the UVeFSW is assumed to behave as an incompressible and single-phase non-Newtonian flow [28-31]. The geometrical model of UVeFSW process is shown in Fig. 2.

The conservation equations of mass and momentum are given as,

$$\frac{\partial \rho}{\partial t} + \nabla \cdot (\rho \vec{v}) = 0 \tag{1}$$

$$\frac{\partial (\rho \vec{v})}{\partial t} + \nabla \cdot (\rho \vec{v} \vec{v}) = -\nabla p + \nabla \cdot \left(\mu (\nabla \vec{v} + \nabla \vec{v}^T)\right) \tag{2}$$

where ρ is density, $\vec{v}$ is material flow velocity, p is fluid pressure, μ is viscosity.

The energy conservation equation is given as,

$$\frac{\partial (\rho H)}{\partial t} + \nabla \cdot (\rho \vec{v} H) = \nabla \cdot (k \nabla T) + S_v \tag{3}$$

where H is enthalpy, k is thermal conductivity, T is temperature, and S_v is the viscous dissipation heat source due to plastic deformation near the tool in the shear zone [5].

Superimposing ultrasonic vibration in FSW, the ultrasonic vibration energy plays two important effects. One is acoustic softening effect, which would affect the dislocation evolution and subsequent reduce the yield stress and flow stress of the plastic deformed materials [32]. The other is the preheating effect due to the vibration friction heat originates from the relative motion between the vibratory sonotrode and the workpiece. In a thermo-fluid model, the fluid viscosity is key to predict the heat and mass transfer in the calculation domain. In the current simulation, the fluid viscosity is defined to be dependent on the temperature, strain rate and ultrasonic vibration energy density, which is proposed in reference [32]. The formulation of the fluid viscosity is given based on the visco-plasticity theory,

$$\mu = \frac{\bar{\sigma}}{3\bar{\dot{\varepsilon}}} \tag{4}$$

$$\bar{\sigma} = \frac{1}{\alpha} ln \left\{ \left[\frac{\bar{\dot{\varepsilon}}}{A} exp\left(\frac{Q}{RT} - \frac{g_0 \mu_m b^3 \beta}{k_B T} \sqrt{\frac{ME}{\hat{\sigma}_{th}}} \right) \right]^{\frac{1}{n}} + \left[1 + \left[\frac{\bar{\dot{\varepsilon}}}{A} exp\left(\frac{Q}{RT} - \frac{g_0 \mu_m b^3 \beta}{k_B T} \sqrt{\frac{ME}{\hat{\sigma}_{th}}} \right) \right]^{\frac{1}{n}} \right]^{\frac{1}{2}} \right\} \quad (5)$$

where $\bar{\sigma}$ is the flow stress, $\bar{\dot{\varepsilon}}$ is the effective strain rate, Q is the activation energy, R is the gas constant, and α, A, n are the material constants which represent the characteristics of base material [32]. g_0 is a pre-factor, μ_m is the temperature-dependent shear modulus [33], b is the magnitude of Burgers vector, M is the Taylor factor, k_B is the Boltzmann's constant, E is the ultrasonic energy density which is calculated using the method proposed in reference [33], $\hat{\sigma}_{th}$ is the thermal components of mechanical threshold stress, β is calibrated parameters for flow stress [32].

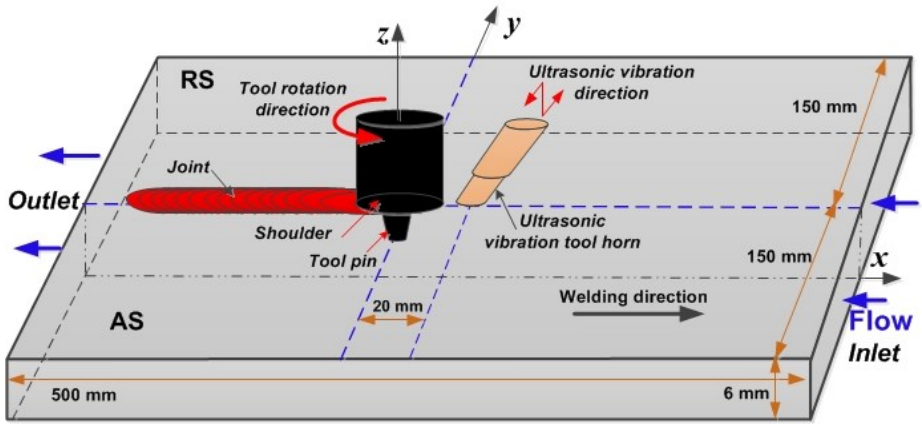

Fig. 2 Geometrical model of ultrasonic vibration enhanced friction stir welding (UVeFSW).

HEAT SOURCE MODEL

The heat source which takes into account the frictional heat at the FSW tool/workpiece contact interfaces as well as the shear plastic deformation heat has been used in this model. The interfacial contact shear stress is defined to be dependent on temperature, strain rate and ultrasonic energy density. Based on the von Mises yield criterion, the interfacial contact shear stress τ_c and interfacial friction stress τ_f at tool-workpiece interface can be expressed as [26]:

$$\tau_c = C_T \frac{\bar{\sigma}}{\sqrt{3}} \quad (6)$$

$$\tau_f = \mu_f P_N \quad (7)$$

where C_T is a temperature-dependent factor at a region near the melting point to prevent overprediction of temperature near the tool during FSW process [26], μ_f is the frictional coefficient, and P_N is the normal pressure at the FSW tool/workpiece contact interface.

Thus, the heat generation rate at FSW tool/workpiece contact interface can be express as:

$$q = \left[\eta(1-\delta)\tau_c + \beta_f \delta \tau_f\right]\left|\vec{v}_t + \vec{U}\right| \tag{8}$$

where η and β_f are the conversion efficiency of plastic deformation and friction heat, respectively. δ is dimensionless slip rate [34]. $\vec{v}_t$ is the interfacial FSW tool velocity vector which is calculated by $\vec{v}_t = \vec{\omega} \times \vec{r}$, and $\vec{\omega}$ is the rotation speed vector, $\vec{r}$ is the radius vector, and $\vec{U}$ is the welding speed vector.

The deformation heat in the shear zone is expressed as a volumetric heat source in the energy conservation equation, which is expressed as [4],

$$S_v = f_m \mu \Phi \tag{9}$$

where f_m is an constant, Φ is a term related to the strain rate of the plastic deformation [4].

The preheating effect originates from the relative frictional sliding between the sonotrode and workpiece, which is considered as a frictional heat flux at the tip of the sonotrode in UVeFSW, is expressed as [26]:

$$q_u = \frac{4\lambda f \mu_c F_c \cos\varphi}{\pi R_h^2} \tag{10}$$

where λ and f are the amplitude and frequency of the ultrasonic, respectively. μ_c is the constant frictional efficiency between sonotrode and workpiece, F_c is the clamping force of the sonotrode, R_h is the radius of the sonotrode at the contact interface with workpiece, φ is the tilt angle of the sonotrode.

Boundary Conditions

The heat dissipation at the top surface of the workpiece involves both convective and radiative heat losses and is expressed as [4-5]:

$$k\frac{\partial T}{\partial \vec{n}} = h_c(T_\infty - T) + \sigma_r \varepsilon_r (T_\infty^4 - T^4) \tag{11}$$

where h_c is the convective heat transfer coefficient, σ_r is the Stefan-Boltzmann constant, ε_r is the external emissivity, and T_∞ is the room temperature.

The bottom and side surfaces of the workpiece are contact to the backplate and clamping equipments. Thus, the boundary condition for heat exchange involves only convective heat transfer:

$$k\frac{\partial T}{\partial \vec{n}} = h_c(T_\infty - T) \tag{12}$$

At the FSW tool/workpiece contact interfaces, the heat flux boundary condition as following is applied [5],

$$k\frac{\partial T}{\partial \vec{n}} = \frac{\sqrt{(k\rho c_p)_w}}{\sqrt{(k\rho c_p)_w}+\sqrt{(k\rho c_p)_t}}q \tag{13}$$

where the subscripts *w* and *t* denote the workpiece and the tool, respectively.

The velocity boundary conditions at the tool-workpiece contact interfaces are expressed in terms of the rotation speed, the welding speed, the dimensionless slip rate and the radius vector as follows [4],

$$\vec{v} = (1-\delta)\vec{\omega}\times\vec{r} + \vec{U} \tag{14}$$

The initial temperature of the material flow and the ambient temperature are assumed to be 300 K. Initially, the plastic material flows in and out of the inlet and outlet boundaries at the welding speed, respectively. The moving wall boundary condition is applied on the other boundaries away from the tool/workpiece contact interfaces. The effect of the threaded pin on material flow is considered as a boundary condition in this study. The thread leads to downward material flow velocity according to the rotation direction of the tool pin and the thread direction [5].

SOLUTION METHOD

Numerical simulation of the process was performed using the computational fluid dynamics (CFD) code, Fluent, based on the governing equations and the boundary conditions as stated above. Conservation principles of mass, momentum and energy were calculated for the incompressible single-phase flow [28]. The calculations of the coupled temperature field and velocity field were performed by the Semi-Implicit Method for Pressure Linked Equations (SIMPLE) algorithms [35]. Second order upwind scheme was used for the discretization of the momentum equations and energy equation. Fig 3 shows the top view of the mesh system for finite volume calculations. Non-uniform grid system was used to discretize the calculation domain. Finer grids were chosen to describe the portion of the domain which encompasses severe material flow and heat generation near the tool and sonotrode, in order to resolve the plasticized material flow and heat convection. The computation was performed until the convergence criteria were reached.

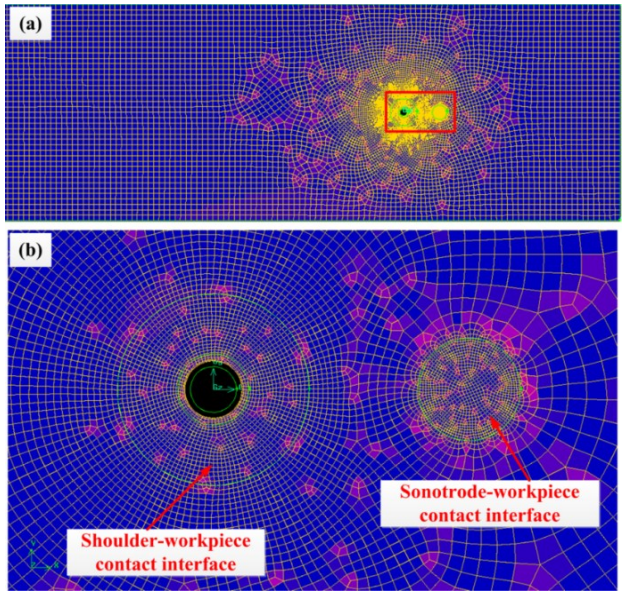

Fig. 3 The mesh system in the simulation. (a) top view of the total workpiece, (b) local view of the mesh near the FSW tool and sonotrode-workpiece contact interface (enlarged of the red area in a).

RESULTS AND DISCUSSION

Fig. 4 shows the monitoring locations on transverse cross-section. Three typical monitor locations near the tool are chosen to output the thermal history during welding process. One located below the tool axis at the bottom of the tool pin (i.e., location M0). The other two located at the top surface of the workpiece and 8.0 mm away from the weld line, with one at the AS (i.e., location M1) and the other at the RS (i.e., location M2).

Fig. 5 shows the calculated temperature fields of FSW and UVeFSW at the top surface of the workpiece and at z = 3.0 (i.e., at the middle of the plate thickness) horizontal plane. It is revealed that the temperature distribution features of FSW and UVeFSW are approximately analogous. Due to superimposing of ultrasonic vibration, the isothermal of the same magnitude in UVeFSW are enlarged ahead of the FSW tool as shown in Fig. 5a and 5c. Fig. 6 shows the calculated temperature fields of the FSW and UVeFSW at transverse cross-section. It is shown that the temperature near the FSW tool in FSW is somehow higher than that in UVeFSW, while there are little temperature difference at about 10 mm away from the weld line.

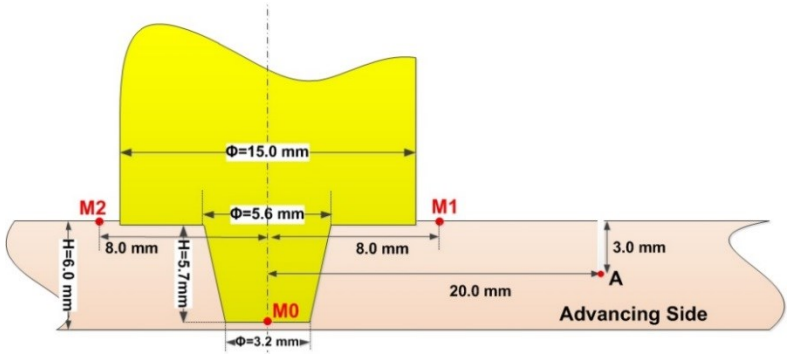

Fig. 4 Schematic figure of the monitoring loations (A, M0, M1 and M2) on transverse cross-section.

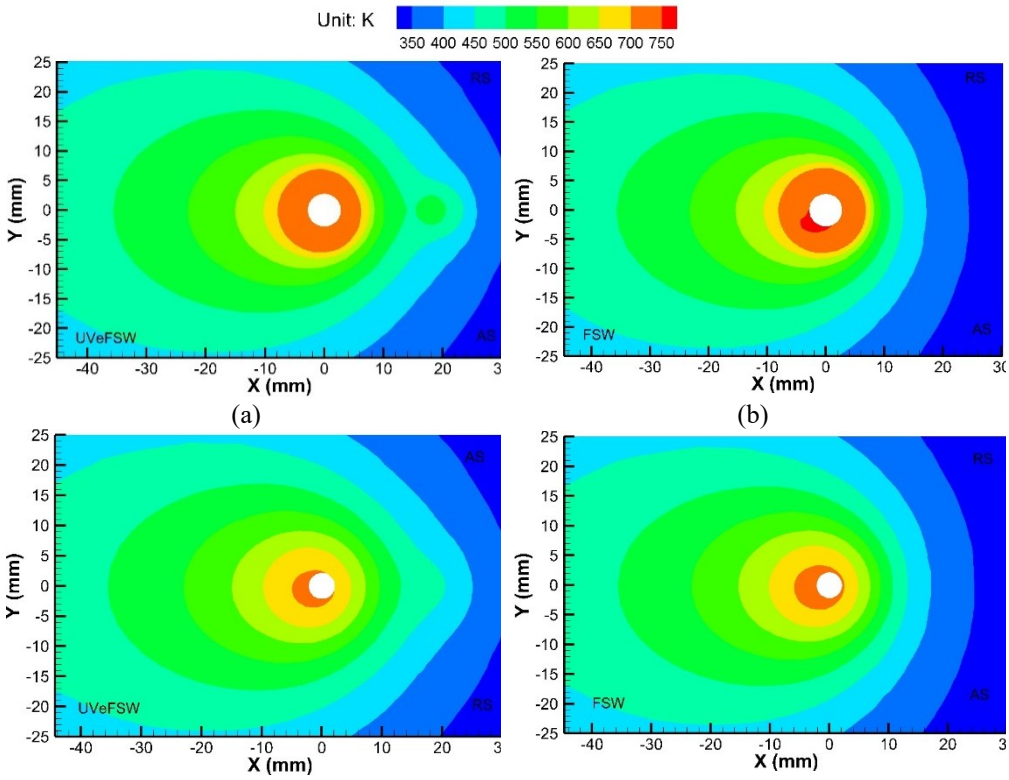

Fig. 5 Predicted temperature field at ω = 600 rpm, U = 240 mm/min. (a) at the top surface of workpiece in UVeFSW; (b) at the top surface of workpiece in FSW; (c) at z = 3 mm plane in UVeFSW; (d) at z = 3 mm plane in FSW.

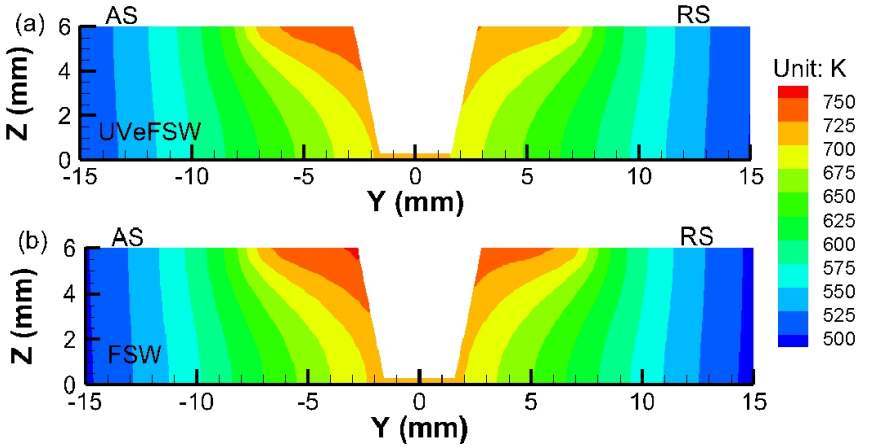

Fig. 6 Predicted temperature field on tranverse cross-section at ω = 600 rpm, U = 240 mm/min. (a) UVeFSW; (b) FSW.

Fig. 7 shows the predicted thermal cycles at three typical locations (i.e., M0, M1 and M2 in Figure 4). It is seen that there is a preheating region near $t = -5$ s (i.e., 20 mm prior to FSW tool axis where the sonotrode located). Fig. 8a shows that the temperature difference between UVeFSW and FSW at the preheating region (i.e., at $t = -5$ s) is ~ 50 K below the tool pin bottom (i.e., at location M0), while the temperature difference decreases to ~20 K at 8.0 mm away from the weld line, as shown in Fig. 8b and 8c. However, there is little temperature difference between the peak temperature in UVeFSW and the one in FSW, the maximum temperature difference at the peak value of thermal cycles is less than 5 K as shown in Fig. 8. From Figs. 5-7, it is clearly shown that the temperature fields in FSW and UVeFSW are approximately analogous. The ultrasonic vibration in FSW does not significant change the process temperature in FSW. This is because on the one hand, the ultrasonic vibration preheats the workpiece at 20 mm before the FSW tool axis, on the other hand, the acoustic softening reduces the strength of plastic material near the tool which resulting in a lower plastic deformation heat generation in UVeFSW. As a result, superimposing ultrasonic vibration in FSW does not cause evident temperature increment.

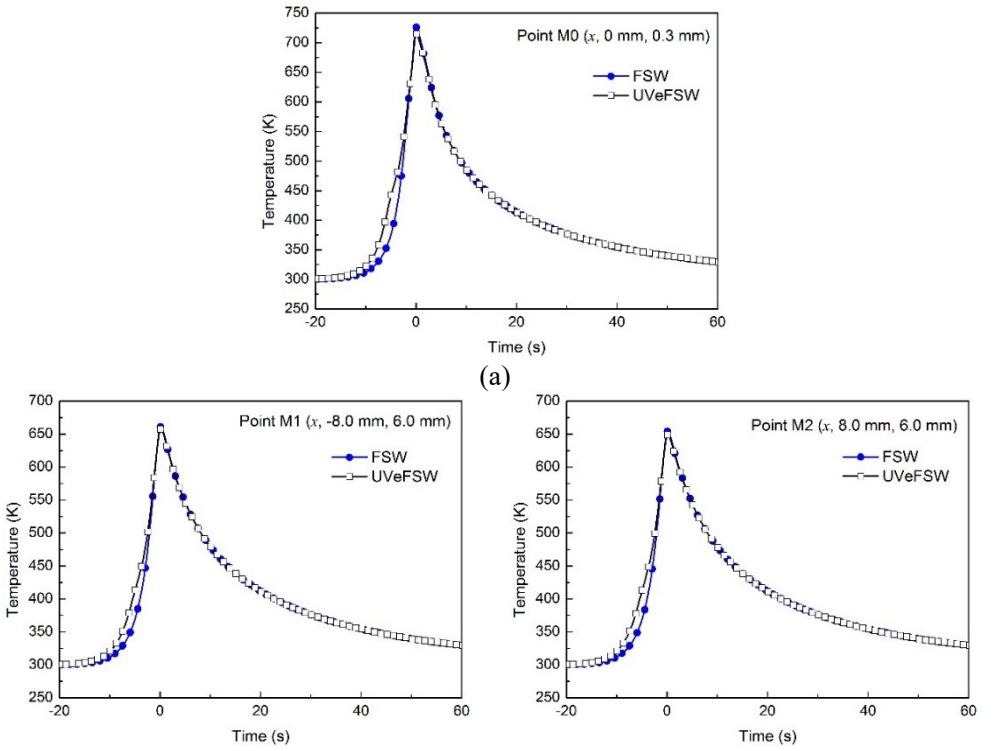

Fig. 7 The calculated thermal cycles in UVeFSW and FSW at ω = 600 rpm, U = 240 mm/min. (a) Location M0; (b) Location M1; (c) Location M2.

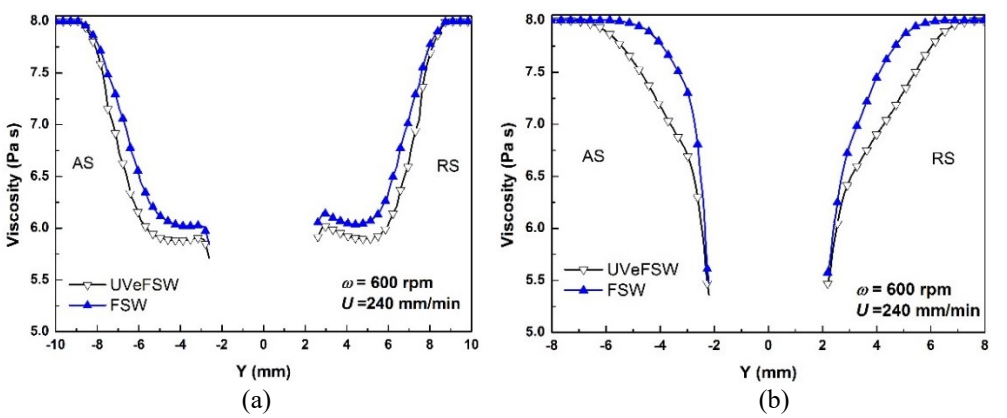

Fig. 8 Variation of viscosity (a) at z = 5 mm and (b) at z = 3 mm horizontal planes in both UVeFSW and FSW (The viscosity value are represented in logarithm to the base 10).

The variation of viscosity near the tool are illustrated in Fig. 8. As pointed out in the literatures [36], the boundary of TMAZ could be obtained by the critical viscosity of 2.5×10^6 Pa·s, because no significant plastic flow occurs above this critical value. Thus, the boundary of iso-viscosity of 2.5×10^6 Pa·s is chosen as the TMAZ boundary as shown in

Fig. 9. Fig. 8 shows that viscosity in UVeFSW is lower than that in FSW, which resulting in a larger TMAZ in UVeFSW (as shown in Fig. 9). It indicates that superimposing ultrasonic vibration on FSW process can enlarge the TMAZ boundaries. This is because the ultrasonic vibration energy reduce the flow stress and the corresponding viscosity value near the tool. As a result, a larger volume of plastic materials near the tool are softened by the acoustic softening effect of the ultrasonic vibration energy which leads to a larger TMAZ in UVeFSW as shown in Fig. 9.

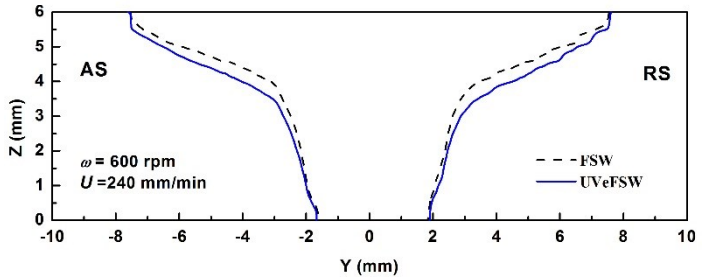

Fig. 9 The calculated iso-viscosity line (2.5×10^6 Pa·s) in UVeFSW and FSW at transverse cross-section

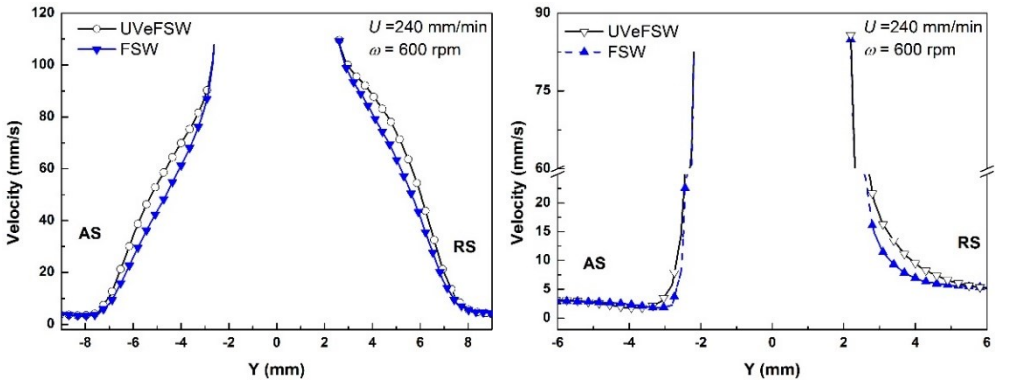

Fig. 10 Variation of material flow velocity (a) at z = 5 mm and (b) at z = 3 mm horizontal planes in both UVeFSW and FSW.

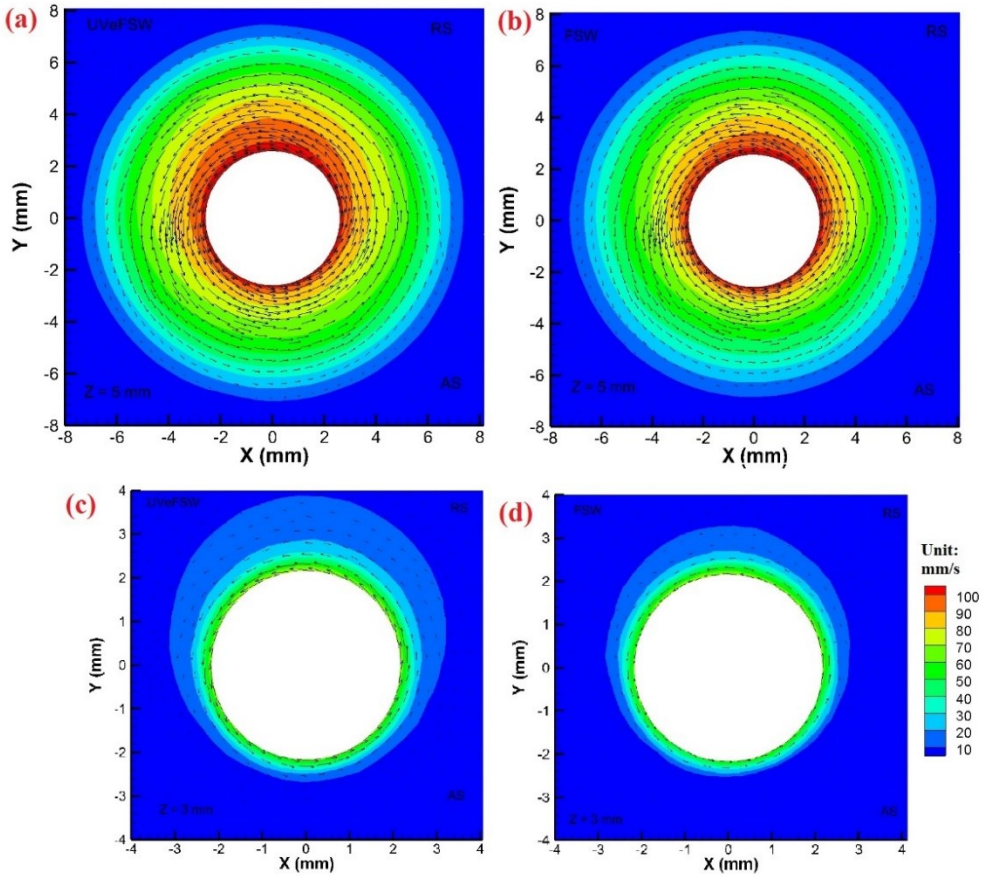

Fig. 11 Material flow at different horizontal plane at ω = 600 rpm, U = 240 mm/min. (a) at z = 5 mm in UVeFSW; (b) at z = 5 mm in FSW; (c) at z = 3 mm in UVeFSW; (d) at z = 3 mm in FSW.

Fig. 10 shows the variation of material flow velocity near the tool in both FSW and UVeFSW. It is clearly shown that the plastic material flow velocity adjacent to the FSW tool is identical in both FSW and UVeFSW. While away from the tool-workpiece interface (i.e., at about 3.0 mm from the weld line at z = 5.0 mm horizontal plane as shown in Fig. 10a and at about 2.5 mm from the weld line at z = 3.0 mm horizontal plane as shown in Fig. 10b), the plastic material flow velocity in UVeFSW is higher than that in FSW. Superimposing ultrasonic vibration in FSW could increase the material flow velocity, especially in the TMAZ. Fig. 11a through 11d illustrates the calculated material flow velocity and vector on horizontal planes at positions Z = 5 and 3 mm from the bottom face, for both FSW and UVeFSW. The plastic material flows round the tool axis in all cases. The rotating flow region decreases with increasing depth, in other word with decreasing Z. This is because the influence of the shoulder decreases when the depth from the top surface increases. However, it can be clearly seen that the contours of the material flow with identical velocity are larger in UVeFSW than those in FSW. The acoustic softening in

UVeFSW leads to a lower viscosity which resulting in an enhancement of plastic material flow near the tool. In addition, the acoustic softening reduce the flow stress which leads to a lower plastic heat generation in UVeFSW and it offsets the preheating effects and resulting in less temperature increment. The exerting ultrasonic vibration can enhance the material flow and the strain rate in the shear layer, but does not cause evident temperature increment, which could be a reason for better mechanical properties of the joints in UVeFSW process.

To validate the model, the experimentally measured macro-sections of welds under welding conditions (800 rpm and 320 mm/min) in UVeFSW was obtained. It was used to compare the calculated TMAZ boundary. It can be found that both are in agreement with each other.

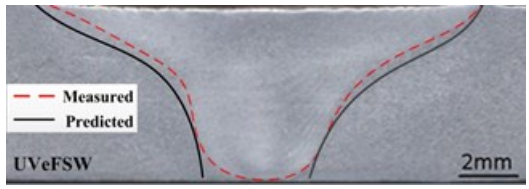

Fig. 12 Comparison of the calculated and measured TMAZ profile in UVeFSW

CONCLUSIONS

A three-dimensional model is developed to conduct the numerical simulation of the material flow and heat transfer in ultrasonic vibration enhanced friction stir welding (UVeFSW) process. Both the effects of ultrasonic softening and preheating are considered in the model. It is found that due to the acoustic softening effect of superimposed ultrasonic vibration energy, the thermo-mechanical affected zone (TMAZ) boundary predicted by iso-viscosity value in UVeFSW are larger than that in conventional FSW process. It reveals that superimposing ultrasonic vibration in FSW can enhance the material flow and the strain rate in the shear layer, but does not cause evident temperature increment. Ultrasonic softening is the mainly function of superimposing ultrasonic vibration in friction stir welding process, while the preheating effect is relatively small. UVeFSW process has great potential to improve the microstructure of joint and reduce the welding force.

ACKNOWLEDGEMENTS

This research was supported by the National Natural Science Foundation of China (Grant No. 51475272).

REFERENCES

[1] P.L. THREADGILL, A.J. LEONARD, H.R. SHERCLIFF, P.J. WITHERS: 'Friction stir welding of aluminium alloys', *International Materials Reviews*, Vol. 54, No. 2, pp. 49-93, 2009.

[2] R. MISHRA, Z.Y. MA: 'Friction stir welding and processing', *Materials Science and Engineering: R*, Vol. 50, No. 1-2, pp. 1-78, 2005.

[3] R. NANDAN, T.S. DEBROY, H.K.D.H. BHADESHIA: 'Recent advances in friction-stir welding-process', weldment structure and properties', *Progress in Materials Science*, Vol. 53, pp. 980-1023, 2008.

[4] A. ARORA, M. MEHTA, A. DE, T. DEBROY: 'Load bearing capacity of tool pin during friction stir welding', *The International Journal of Advanced Manufacturing Technology*, Vol. 61, No. 9-12, pp. 911-920, 2012.

[5] G. CAM: 'Friction stir welded structural materials: beyond Al-alloys', *International Materials Reviews*, Vol. 56, No. 1, pp.1-48, 2011.

[6] G. KOHN, Y. GREENBERG, I. MAKOVER, A. MUNITZ: 'Laser-assisted friction stir welding', *Welding Journal*, Vol. 81, No. 2, pp. 46-46, 2002.

[7] J. LUO, W. CHEN, G. FU: 'Hybrid-heat effects on electrical-current aided friction stir welding of steel, and Al and Mg alloys', *Journal of Materials Processing Technology*, Vol. 214, No. 12, pp. 3002-3012, 2014.

[8] A.H. LOTFI, S. NOUROUZI: 'Predictions of the optimized friction stir welding process parameters for joining AA7075-T6 aluminum alloy using preheating system', *The International Journal of Advanced Manufacturing Technology*, Vol. 73, No. 9-12, pp. 1117-1137, 2014.

[9] X.C. LIU, C.S. WU, G.K. PADHY: 'Characterization of plastic deformation and material flow in ultrasonic vibration enhanced friction stir welding', *Scripta Materialia*, Vol. 102, pp. 95-98, 2015.

[10] K. PARK: *Development and analysis of ultrasonic assisted friction stir welding process*. PhD Thesis, University of Michigan, 2009.

[11] O. IZUMI, K. OYAMA, Y. SUZUKI: 'Effects of superimposed ultrasonic vibration on compressive deformation of metals', *Transactions of the Japan Institute of Metals*, Vol. 7, No. 3, pp. 162-167, 1966.

[12] Y. DAUD, M. LUCAS, Z. HUANG: 'Modelling the effects of superimposed ultrasonic vibrations on tension and compression tests of aluminium', *Journal of Materials Processing Technology*, Vol. 186, No. 1, pp. 179-190, 2007.

[13] A. SIDDIQ, T. EL SAYED: 'Ultrasonic-assisted manufacturing processes: Variational model and numerical simulations', *Ultrasonics*, Vol. 52, No. 4, pp. 521-529, 2012.

[14] S. AMINI, M.R. AMIRI: 'Study of ultrasonic vibrations' effect on friction stir welding', *The International Journal of Advanced Manufacturing Technology*, Vol. 73, No. 1-4, pp. 127-135, 2014.

[15] H.K. MA, D.Q. HE, J.S. LIU: 'Ultrasonically assisted friction stir welding of aluminium alloy 6061', *Science and Technology of Welding and Joining*, Vol. 20, No. 3, pp. 216-221, 2015.

[16] Y. ROSTAMIYAN, A. SEIDANLOO, H. SOHRABPOOR, R. TEIMOURI: 'Experimental studies on ultrasonically assisted friction stir spot welding of AA6061', *Archives of Civil and Mechanical Engineering*, Vol. 15, No. 2, pp. 335-346, 2015.

[17] M. AHMADNIA, A. SEIDANLOO, R. TEIMOURI, Y. ROSTAMIYAN, K.G. TITRASHI: 'Determining influence of ultrasonic-assisted friction stir welding parameters on mechanical and tribological properties of AA6061 joints', *The International Journal of Advanced Manufacturing Technology*, Vol. 78, No. 9-12, pp. 2009-2024, 2015.

[18] Y.B. ZHONG, C.S. WU, G.K. PADHY: 'Effect of ultrasonic vibration on welding load, temperature and material flow in friction stir welding', *Journal of Materials Processing Technology*, Vol. 239, pp. 273-283, 2017.

[19] X. HE, F. GU, A. BALL: 'A review of numerical analysis of friction stir welding', *Progress in Materials Science*, Vol. 65, pp. 1-66, 2014.
[20] G. CHEN, Q. SHI, Y. LI, Y. SUN, Q. DAI, J. JIA, Y. ZHU, J. WU: 'Computational fluid dynamics studies on heat generation during friction stir welding of aluminum alloy', *Computational Materials Science*, 2013, 79: 540-546.
[21] L. SHI, C.S. WU: 'Transient model of heat transfer and material flow at different stages of friction stir welding process', *Journal of Manufacturing Processes*, Vol. 25, pp. 323-339, 2017.
[22] R.L. LAI, D.Q. HE, L.C. LIU, S.Y. YE, K.Y. YANG: 'A study of the temperature field during ultrasonic-assisted friction-stir welding', *The International Journal of Advanced Manufacturing Technology*, Vol. 73, No. 1-4, pp. 321-327, 2014.
[23] J.C. HUNG, C. HUNG: 'The influence of ultrasonic-vibration on hot upsetting of aluminum alloy', *Ultrasonics*, Vol. 43, No. 8, pp. 692-698, 2005.
[24] A. SIDDIQ, T. EL SAYED: 'Acoustic softening in metals during ultrasonic assisted deformation via CP-FEM', *Materials Letters*, Vol. 65, No. 2, pp. 356-359, 2011.
[25] G.S. KELLY, S.G. ADVANI, J.W. GILLESPIE, T.A. BOGETTI: 'A model to characterize acoustic softening during ultrasonic consolidation', *Journal of Materials Processing Technology*, Vol. 213, No. 11, pp. 1835-1845, 2013.
[26] L. SHI, C.S. WU, Z. SUN: 'An integrated model for analysing the effects of ultrasonic vibration on tool torque and thermal processes in friction stir welding', *Science and Technology of Welding and Joining*, Vol. 23, No. 5, pp. 365-379, 2018.
[27] L. SHI, C.S WU, S. GAO: 'Analysis of welding load reduction in ultrasonic vibration-enhanced friction stir welding', *The International Journal of Advanced Manufacturing Technology*, 2018. https://doi.org/10.1007/s00170-018-2472-1.
[28] R. NANDAN, G.G. ROY, T. DEBROY: 'Three-dimensional heat and material flow during friction stir welding of mild steel', *Acta Materialia*, Vol. 55, No. 3, pp. 883-895, 2007.
[29] H.H. CHO, S.T. HONG, J.H. ROH, H.S. CHOI, S.H. KANG, R.J. STEEL, H.N. HAN: 'Three-dimensional numerical and experimental investigation on friction stir welding processes of ferritic stainless steel', *Acta Materialia*, Vol. 61, No. 7, pp. 2649-2661, 2013.
[30] L. SHI, C.S. WU, H.J. LIU: 'Numerical analysis of heat generation and temperature field in reverse dual-rotation friction stir welding', *The International Journal of Advanced Manufacturing Technology*, Vol. 74, No. 1-4, pp. 319-334, 2014.
[31] A. ARORA, A. DE, T. DEBROY: 'Toward optimum friction stir welding tool shoulder diameter', *Scripta Materialia*, Vol. 64, No. 1, pp. 9-12, 2011.
[32] L. SHI, C.S. WU, S. GAO, G.K. PADHY: 'Modified constitutive equation for use in modeling the ultrasonic vibration enhanced friction stir welding process', *Scripta Materialia*, Vol. 119, pp. 21-26, 2016.
[33] L. SHI, C.S. WU, G.K. PADHY, S. GAO: 'Numerical simulation of ultrasonic field and its acoustoplastic influence on friction stir welding', *Materials & Design*, Vol. 104, pp. 102-115, 2016.
[34] R. NANDAN, G.G. ROY, T. DEBROY: 'Numerical simulation of three-dimensional heat transfer and plastic flow during friction stir welding', *Metallurgical and Materials Transactions A*, Vol. 37, No. 4, pp. 1247-1259, 2006.
[35] S.V. PATANKAR: '*Numerical Heat Transfer and Fluid Flow*', Hemisphere, Washington, D.C., USA. 1980.
[36] L. SHI, C.S. WU, H.J. LIU: 'The effect of the welding parameters and tool size on the thermal process and tool torque in reverse dual-rotation friction stir welding', *International Journal of Machine Tools and Manufacture*, Vol. 91, pp. 1-11, 2015.